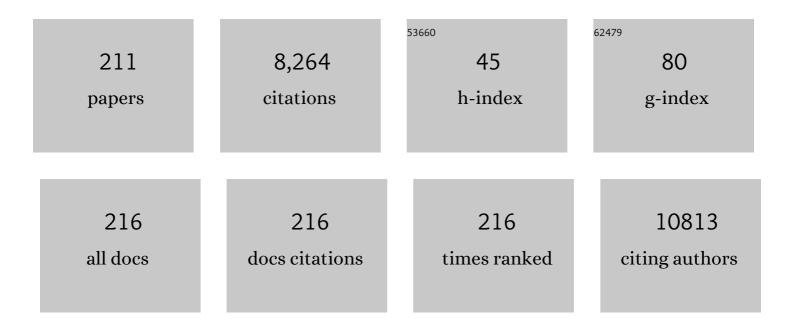
## **Giuseppe Portale**

List of Publications by Year in descending order

Source: https://exaly.com/author-pdf/4742844/publications.pdf Version: 2024-02-01



#	Article	IF	CITATIONS
1	Dynamic Control of a Multistate Chiral Supramolecular Polymer in Water. Journal of the American Chemical Society, 2022, 144, 6019-6027.	6.6	36
2	Highâ€Performance Organic Electrochemical Transistors and Neuromorphic Devices Comprising Naphthalenediimideâ€Dialkoxybithiazole Copolymers Bearing Glycol Ether Pendant Groups. Advanced Functional Materials, 2022, 32, .	7.8	33
3	Film formation mechanism uncovered in 2D/3D mixed-dimensional lead halide perovskites. CheM, 2022, 8, 899-902.	5.8	0
4	A light-fuelled nanoratchet shifts a coupled chemical equilibrium. Nature Nanotechnology, 2022, 17, 159-165.	15.6	41
5	Structural Dynamics and Tunability for Colloidal Tin Halide Perovskite Nanostructures. Advanced Materials, 2022, 34, e2201353.	11.1	16
6	Tin-lead-metal halide perovskite solar cells with enhanced crystallinity and efficiency by addition of fluorinated long organic cation. Applied Physics Reviews, 2022, 9, .	5.5	13
7	Confined crystallization and polymorphism in iPP thin films. Polymer, 2022, 255, 125126.	1.8	1
8	Reversibly Photoâ€Modulating Mechanical Stiffness and Toughness of Bioengineered Protein Fibers. Angewandte Chemie, 2021, 133, 3259-3265.	1.6	8
9	Amphipathic Side Chain of a Conjugated Polymer Optimizes Dopant Location toward Efficient Nâ€Type Organic Thermoelectrics. Advanced Materials, 2021, 33, e2006694.	11.1	91
10	Reversibly Photoâ€Modulating Mechanical Stiffness and Toughness of Bioengineered Protein Fibers. Angewandte Chemie - International Edition, 2021, 60, 3222-3228.	7.2	25
11	Solution-processing of semiconducting organic small molecules: what we have learnt from 5,11-bis(triethylsilylethynyl)anthradithiophene. Journal of Materials Chemistry C, 2021, 9, 10547-10556.	2.7	11
12	Field‣ffect Transistors Based on Formamidinium Tin Triiodide Perovskite. Advanced Functional Materials, 2021, 31, 2008478.	7.8	44
13	Proton conducting ABA triblock copolymers with sulfonated poly(phenylene sulfide sulfone) midblock obtained via copper-free thiol-click chemistry. Polymer Chemistry, 2021, 12, 2563-2571.	1.9	3
14	Fullerene derivatives with oligoethylene–glycol side chains: an investigation on the origin of their outstanding transport properties. Journal of Materials Chemistry C, 2021, 9, 16217-16225.	2.7	10
15	Influence of the stoichiometry of tin-based 2D/3D perovskite active layers on solar cell performance. Journal of Materials Chemistry A, 2021, 9, 10095-10103.	5.2	13
16	Self-Organized Tailoring of Faceted Glass Nanowrinkles for Organic Nanoelectronics. ACS Applied Nano Materials, 2021, 4, 1940-1950.	2.4	11
17	Boosting the Thermoelectric Properties of PEDOT:PSS via Lowâ€Impact Deposition of Tin Oxide Nanoparticles. Advanced Electronic Materials, 2021, 7, 2001284.	2.6	13
18	Structural Transitions During Formation and Rehydration of Proton Conducting Polymeric Membranes. Macromolecular Rapid Communications, 2021, 42, 2000717.	2.0	0

#	Article	IF	CITATIONS
19	Engineering the Thermoelectrical Properties of PEDOT:PSS by Alkali Metal Ion Effect. Engineering, 2021, 7, 647-654.	3.2	7
20	Molecular Doping Directed by a Neutral Radical. ACS Applied Materials & Interfaces, 2021, 13, 29858-29865.	4.0	12
21	Scalable, Template Driven Formation of Highly Crystalline Leadâ€īn Halide Perovskite Films. Advanced Functional Materials, 2021, 31, 2105734.	7.8	22
22	Ionic thermoelectric materials for waste heat harvesting. Colloid and Polymer Science, 2021, 299, 465-479.	1.0	16
23	Crystallization driven boost in fill factor and stability in additive-free organic solar cells. Journal of Materials Chemistry A, 2021, 9, 23783-23792.	5.2	11
24	Revisiting the Mechanism of the Meso-to-α Transition of Isotactic Polypropylene and Ethylene–Propylene Random Copolymers. Macromolecules, 2021, 54, 9681-9691.	2.2	2
25	Data Mining of Polymer Phase Transitions upon Temperature Changes by Small and Wide-Angle X-ray Scattering Combined with Raman Spectroscopy. Polymers, 2021, 13, 4203.	2.0	3
26	Tuning the Energetic Landscape of Ruddlesden–Popper Perovskite Films for Efficient Solar Cells. ACS Energy Letters, 2020, 5, 39-46.	8.8	47
27	Stable Cesium Formamidinium Lead Halide Perovskites: A Comparison of Photophysics and Phase Purity in Thin Films and Single Crystals. Energy Technology, 2020, 8, 1901041.	1.8	19
28	Intermolecular channels direct crystal orientation in mineralized collagen. Nature Communications, 2020, 11, 5068.	5.8	90
29	DNA Self-Assembly Mediated by Programmable Soft-Patchy Interactions. ACS Nano, 2020, 14, 13524-13535.	7.3	6
30	Rapid Self-Assembly and Sequential Infiltration Synthesis of High χ Fluorine-Containing Block Copolymers. Macromolecules, 2020, 53, 6246-6254.	2.2	10
31	De novo rational design of a freestanding, supercharged polypeptide, proton-conducting membrane. Science Advances, 2020, 6, eabc0810.	4.7	24
32	Unraveling the Microstructure of Layered Metal Halide Perovskite Films. Small Structures, 2020, 1, 2000074.	6.9	8
33	Contribution of Ex-Situ and In-Situ X-ray Grazing Incidence Scattering Techniques to the Understanding of Quantum Dot Self-Assembly: A Review. Nanomaterials, 2020, 10, 2240.	1.9	8
34	N-type organic thermoelectrics: demonstration of ZT > 0.3. Nature Communications, 2020, 11, 5694.	5.8	98
35	On the Colloidal Stability of PbS Quantum Dots Capped with Methylammonium Lead Iodide Ligands. ACS Applied Materials & Interfaces, 2020, 12, 52959-52966.	4.0	17
36	Systematic Investigation on the Structure-Property Relationship in Isotactic Polypropylene Films Processed via Cast Film Extrusion. Polymers, 2020, 12, 1636.	2.0	14

#	Article	IF	CITATIONS
37	Role of the Processing Solvent on the Electrical Conductivity of PEDOT:PSS. Advanced Materials Interfaces, 2020, 7, 2000641.	1.9	53
38	Highly Stable Membranes of Poly(phenylene sulfide benzimidazole) Cross-Linked with Polyhedral Oligomeric Silsesquioxanes for High-Temperature Proton Transport. ACS Applied Energy Materials, 2020, 3, 7873-7884.	2.5	21
39	Surface mobility and impact of precursor dosing during atomic layer deposition of platinum: <i>in situ</i> monitoring of nucleation and island growth. Physical Chemistry Chemical Physics, 2020, 22, 24917-24933.	1.3	19
40	Structural characterization of supramolecular hollow nanotubes with atomistic simulations and SAXS. Physical Chemistry Chemical Physics, 2020, 22, 21083-21093.	1.3	14
41	Photochromism in Ruddlesden–Popper copper-based perovskites: a light-induced change of coordination number at the surface. Journal of Materials Chemistry C, 2020, 8, 15377-15384.	2.7	14
42	Molecular packing structure of fibrin fibers resolved by X-ray scattering and molecular modeling. Soft Matter, 2020, 16, 8272-8283.	1.2	13
43	Can Ferroelectricity Improve Organic Solar Cells?. Macromolecular Rapid Communications, 2020, 41, e2000124.	2.0	4
44	Supramolecular Polymer Brushes: Influence of Molecular Weight and Cross-Linking on Linear Viscoelastic Behavior. Macromolecules, 2020, 53, 4810-4820.	2.2	4
45	Impact of the Hole Transport Layer on the Charge Extraction of Ruddlesden–Popper Perovskite Solar Cells. ACS Applied Materials & Interfaces, 2020, 12, 29505-29512.	4.0	4
46	Crystal Formation: Mechanism of Crystal Formation in Ruddlesden–Popper Snâ€Based Perovskites (Adv.) Tj ET	Qq0 0 0 r 7.8	gBŢ /Overlock
47	Novel engineered proteins for mechanomaterials. Frontiers of Chemical Science and Engineering, 2020, 14, 1122-1123.	2.3	Ο
48	Mechanism of Crystal Formation in Ruddlesden–Popper Snâ€Based Perovskites. Advanced Functional Materials, 2020, 30, 2001294.	7.8	91
49	Order–disorder transition in supramolecular polymer combs/brushes with polymeric side chains. Polymer Chemistry, 2020, 11, 2749-2760.	1.9	5
50	Lithium and magnesium polymeric electrolytes prepared using poly(glycidyl ether)-based polymers with short grafted chains. Polymer Chemistry, 2020, 11, 2070-2079.	1.9	6
51	Thiol-free self-assembled oligoethylene glycols enable robust air-stable molecular electronics. Nature Materials, 2020, 19, 330-337.	13.3	60
52	Fabrication of highly ordered Cu2+/Fe3+ decorated polyhedral oligomeric silsesquioxane hybrids: How metal coordination influences structure. Journal of Colloid and Interface Science, 2020, 572, 207-215.	5.0	2
53	Electrical Conductivity of Doped Organic Semiconductors Limited by Carrier–Carrier Interactions. ACS Applied Materials & Interfaces, 2020, 12, 56222-56230.	4.0	32
54	Tailoring block copolymer nanoporous thin films with acetic acid as a small guest molecule. Polymer International, 2019, 68, 1914-1920.	1.6	4

#	Article	IF	CITATIONS
55	Doping Engineering Enables Highly Conductive and Thermally Stable n-Type Organic Thermoelectrics with High Power Factor. ACS Applied Energy Materials, 2019, 2, 6664-6671.	2.5	38
56	Improved energy density and charge-discharge efficiency in solution processed highly defined ferroelectric block copolymer-based dielectric nanocomposites. Nano Energy, 2019, 64, 103939.	8.2	17
57	Chemical Solution Deposition of Ordered 2D Arrays of Room-Temperature Ferrimagnetic Cobalt Ferrite Nanodots. Polymers, 2019, 11, 1598.	2.0	7
58	Investigation of the Nanoscale Morphology in Industrially Relevant Clearcoats of Waterborne Polymer Colloids by Means of Variable-Angle Grazing Incidence Small-Angle X-ray Scattering. ACS Applied Polymer Materials, 2019, 1, 2482-2494.	2.0	6
59	Electrostatically PEGylated DNA enables salt-free hybridization in water. Chemical Science, 2019, 10, 10097-10105.	3.7	9
60	Supramolecular Mimic for Bottlebrush Polymers in Bulk. ACS Omega, 2019, 4, 16481-16492.	1.6	12
61	Monitoring morphology evolution within block copolymer microparticles during dispersion polymerisation in supercritical carbon dioxide: a high pressure SAXS study. Polymer Chemistry, 2019, 10, 860-871.	1.9	20
62	Physical pinning and chemical crosslinking-induced relaxor ferroelectric behavior in P(VDF- <i>ter</i> -TrFE- <i>ter</i> -VA) terpolymers. Journal of Materials Chemistry A, 2019, 7, 2795-2803.	5.2	17
63	Overcoming Coulomb Interaction Improves Free-Charge Generation and Thermoelectric Properties for n-Doped Conjugated Polymers. ACS Energy Letters, 2019, 4, 1556-1564.	8.8	110
64	Bicontinuous Network Nanostructure with Tunable Thickness Formed on Asymmetric Triblock Terpolymer Thick Films. Macromolecules, 2019, 52, 4413-4420.	2.2	10
65	Energy level modulation of ITIC derivatives: Effects on the photodegradation of conventional and inverted organic solar cells. Organic Electronics, 2019, 69, 255-262.	1.4	31
66	Enhancing the crystallinity and perfecting the orientation of formamidinium tin iodide for highly efficient Sn-based perovskite solar cells. Nano Energy, 2019, 60, 810-816.	8.2	140
67	A Photoaddressable Liquid Crystalline Phase Transition in Graphene Oxide Nanocomposites. Advanced Functional Materials, 2019, 29, 1900738.	7.8	2
68	Improved photostability in ternary blend organic solar cells: the role of [70]PCBM. Journal of Materials Chemistry C, 2019, 7, 5104-5111.	2.7	46
69	Favorable Mixing Thermodynamics in Ternary Polymer Blends for Realizing High Efficiency Plastic Solar Cells. Advanced Energy Materials, 2019, 9, 1803394.	10.2	44
70	Cytoskeletal stiffening in synthetic hydrogels. Nature Communications, 2019, 10, 609.	5.8	63
71	Electroactive materials with tunable response based on block copolymer self-assembly. Nature Communications, 2019, 10, 601.	5.8	44
72	Pronounced Surface Effects on the Curie Transition Temperature in Nanoconfined P(VDF-TrFE) Crystals. Macromolecules, 2019, 52, 1567-1576.	2.2	12

#	Article	IF	CITATIONS
73	In situ observation of synthesized nanoparticles in ultra-dilute aerosols via X-ray scattering. Nano Research, 2019, 12, 25-31.	5.8	9
74	Tailored Self-Assembled Ferroelectric Polymer Nanostructures with Tunable Response. Macromolecules, 2019, 52, 354-364.	2.2	12
75	Micellarâ€Mediated Block Copolymer Ordering Dynamics Revealed by In Situ Grazing Incidence Smallâ€Angle Xâ€Ray Scattering during Spin Coating. Advanced Functional Materials, 2019, 29, 1806741.	7.8	13
76	Mechanistic insights in Zr- and Hf-based molecular hybrid EUV photoresists. Journal of Micro/ Nanolithography, MEMS, and MOEMS, 2019, 18, 1.	1.0	21
77	Operando SAXS/WAXS on the a-P/C as the Anode for Na-Ion Batteries. Journal of Physical Chemistry C, 2018, 122, 5917-5923.	1.5	10
78	Genetically Engineered Supercharged Polypeptide Fluids: Fast and Persistent Selfâ€Ordering Induced by Touch. Angewandte Chemie - International Edition, 2018, 57, 6878-6882.	7.2	38
79	Enhancing Molecular nâ€Type Doping of Donor–Acceptor Copolymers by Tailoring Side Chains. Advanced Materials, 2018, 30, 1704630.	11.1	217
80	Porphyrin/sPEEK Membranes with Improved Conductivity and Durability for PEFC Technology. ACS Applied Energy Materials, 2018, 1, 1664-1673.	2.5	16
81	Highly Reproducible Snâ€Based Hybrid Perovskite Solar Cells with 9% Efficiency. Advanced Energy Materials, 2018, 8, 1702019.	10.2	726
82	Nâ€Type Organic Thermoelectrics of Donor–Acceptor Copolymers: Improved Power Factor by Molecular Tailoring of the Density of States. Advanced Materials, 2018, 30, e1804290.	11.1	161
83	Complex strain induced structural changes observed in fibrin assembled in human plasma. Nanoscale, 2018, 10, 10063-10072.	2.8	7
84	Enhancing the ferroelectric performance of P(VDF-co-TrFE) through modulation of crystallinity and polymorphism. Polymer, 2018, 149, 66-72.	1.8	28
85	Side-chain effects on N-type organic thermoelectrics: A case study of fullerene derivatives. Nano Energy, 2018, 52, 183-191.	8.2	45
86	Enhancing the Performance of the Half Tin and Half Lead Perovskite Solar Cells by Suppression of the Bulk and Interfacial Charge Recombination. Advanced Materials, 2018, 30, e1803703.	11.1	65
87	Solar Cells: Enhancing the Performance of the Half Tin and Half Lead Perovskite Solar Cells by Suppression of the Bulk and Interfacial Charge Recombination (Adv. Mater. 35/2018). Advanced Materials, 2018, 30, 1870263.	11.1	0
88	Ti, Zr, and Hf-based molecular hybrid materials as EUV photoresists. , 2018, , .		5
89	Surface induced orientation and vertically layered morphology in thin films of poly(3-hexylthiophene) crystallized from the melt. Journal of Materials Research, 2017, 32, 1957-1968.	1.2	22
90	Templated Subâ€100â€nmâ€Thick Doubleâ€Gyroid Structure from Siâ€Containing Block Copolymer Thin Films. Small, 2017, 13, 1603777.	5.2	16

#	Article	IF	CITATIONS
91	Independent tuning of size and coverage of supported Pt nanoparticles using atomic layer deposition. Nature Communications, 2017, 8, 1074.	5.8	95
92	Subâ€Micrometer Structure Formation during Spin Coating Revealed by Timeâ€Resolved In Situ Laser and Xâ€Ray Scattering. Advanced Functional Materials, 2017, 27, 1702516.	7.8	35
93	Nâ€Type Organic Thermoelectrics: Improved Power Factor by Tailoring Host–Dopant Miscibility. Advanced Materials, 2017, 29, 1701641.	11.1	131
94	Nematic DNA Thermotropic Liquid Crystals with Photoresponsive Mechanical Properties. Small, 2017, 13, 1701207.	5.2	32
95	On the Dimensional Control of 2 D Hybrid Nanomaterials. Chemistry - A European Journal, 2017, 23, 12534-12541.	1.7	4
96	Fabrication and Postmodification of Nanoporous Liquid Crystalline Networks via Dynamic Covalent Chemistry. Chemistry of Materials, 2017, 29, 6601-6605.	3.2	22
97	Formation and growth of palladium nanoparticles inside porous poly(4-vinyl-pyridine) monitored by operando techniques: The role of different reducing agents. Catalysis Today, 2017, 283, 144-150.	2.2	8
98	Anisotropic Lithium Ion Conductivity in Singleâ€lon Diblock Copolymer Electrolyte Thin Films. Macromolecular Rapid Communications, 2016, 37, 221-226.	2.0	7
99	Mobile setup for synchrotron based <i>in situ</i> characterization during thermal and plasma-enhanced atomic layer deposition. Review of Scientific Instruments, 2016, 87, 113905.	0.6	21
100	Bulk heterojunction morphology of polymer:fullerene blends revealed by ultrafast spectroscopy. Scientific Reports, 2016, 6, 36236.	1.6	19
101	Pd nanoparticles formation inside porous polymeric scaffolds followed by <i>in situ</i> XANES/SAXS. Journal of Physics: Conference Series, 2016, 712, 012039.	0.3	1
102	Archimedean Tilings and Hierarchical Lamellar Morphology Formed by Semicrystalline Miktoarm Star Terpolymer Thin Films. ACS Nano, 2016, 10, 4055-4061.	7.3	21
103	Polymer research and synchrotron radiation perspectives. European Polymer Journal, 2016, 81, 415-432.	2.6	16
104	The evolution of bicontinuous polymeric nanospheres in aqueous solution. Soft Matter, 2016, 12, 4113-4122.	1.2	19
105	Accelerated growth from amorphous clusters to metallic nanoparticles observed in electrochemical deposition of platinum within nanopores of porous silicon. Electrochemistry Communications, 2016, 71, 9-12.	2.3	10
106	Bundle Formation in Biomimetic Hydrogels. Biomacromolecules, 2016, 17, 2642-2649.	2.6	47
107	Smectic phase in suspensions of gapped DNA duplexes. Nature Communications, 2016, 7, 13358.	5.8	38
108	Structurally-driven Enhancement of Thermoelectric Properties within Poly(3,4-ethylenedioxythiophene) thin Films. Scientific Reports, 2016, 6, 30501.	1.6	67

#	Article	IF	CITATIONS
109	Melt-Miscible Oxalamide Based Nucleating Agents and Their Nucleation Efficiency in Isotactic Polypropylene. Industrial & Engineering Chemistry Research, 2016, 55, 11756-11766.	1.8	14
110	Tuning Ordered Pattern of Pd Species through Controlled Block Copolymer Self-Assembly. Journal of Physical Chemistry B, 2016, 120, 6829-6841.	1.2	6
111	Molecular ordering in the high-temperature nematic phase of an all-aromatic liquid crystal. Soft Matter, 2016, 12, 2309-2314.	1.2	10
112	How does dense phase CO <sub>2</sub> influence the phase behaviour of block copolymers synthesised by dispersion polymerisation?. Polymer Chemistry, 2016, 7, 905-916.	1.9	25
113	Improving Stiffness, Strength, and Toughness of Poly(ω-pentadecalactone) Fibers through <i>in Situ</i> Reinforcement with a Vanillic Acid-Based Thermotropic Liquid Crystalline Polyester. Macromolecules, 2016, 49, 2228-2237.	2.2	17
114	Structure evolution during film blowing: An experimental study using in-situ small angle X-ray scattering. European Polymer Journal, 2016, 74, 190-208.	2.6	34
115	Combining Fast Scanning Chip Calorimetry with Structural and Morphological Characterization Techniques. , 2016, , 327-359.		9
116	Real-Time Fast Structuring of Polymers Using Synchrotron WAXD/SAXS Techniques. Advances in Polymer Science, 2015, , 127-165.	0.4	11
117	Simultaneous Synchrotron WAXD and Fast Scanning (Chip) Calorimetry: On the (Isothermal) Crystallization of HDPE and PA11 at High Supercoolings and Cooling Rates up to 200 ŰC s <sup>â'`1</sup> . Macromolecular Rapid Communications, 2015, 36, 1184-1191.	2.0	44
118	Microfluidic Assisted Selfâ€Assembly of pHâ€Sensitive Lowâ€Molecular Weight Hydrogelators Close to the Minimum Gelation Concentration. Macromolecular Symposia, 2015, 358, 59-66.	0.4	4
119	The Pyridyl Functional Groups Guide the Formation of Pd Nanoparticles Inside A Porous Poly(4â€Vinylâ€Pyridine). ChemCatChem, 2015, 7, 2188-2195.	1.8	15
120	Photoresponsive Nanoporous Smectic Liquid Crystalline Polymer Networks: Changing the Number of Binding Sites and Pore Dimensions in Polymer Adsorbents by Light. Macromolecules, 2015, 48, 4073-4080.	2.2	29
121	About the Interactions Controlling Nafion's Viscoelastic Properties and Morphology. Macromolecules, 2015, 48, 8534-8545.	2.2	22
122	Testing the Vesicular Morphology to Destruction: Birth and Death of Diblock Copolymer Vesicles Prepared via Polymerization-Induced Self-Assembly. Journal of the American Chemical Society, 2015, 137, 1929-1937.	6.6	168
123	Induced Chirality in Confined Space on Halogen Gold Complexes. Journal of Physical Chemistry C, 2015, 119, 18798-18807.	1.5	3
124	Understanding the unusual reorganization of the nanostructure of a dark conglomerate phase. Physical Review E, 2015, 91, 042504.	0.8	22
125	Unusual Melting Behavior in Flow Induced Crystallization of LLDPE: Effect of Pressure. Macromolecules, 2015, 48, 2551-2560.	2.2	20
126	Synthesis, Thermal Processing, and Thin Film Morphology of Poly(3-hexylthiophene)–Poly(styrenesulfonate) Block Copolymers. Macromolecules, 2015, 48, 2107-2117.	2.2	46

#	Article	IF	CITATIONS
127	<i>In Situ</i> Monitoring of Laser-Induced Periodic Surface Structures Formation on Polymer Films by Grazing Incidence Small-Angle X-ray Scattering. Langmuir, 2015, 31, 3973-3981.	1.6	29
128	The effects of lateral halogen substituents on the low-temperature cybotactic nematic phase in oxadiazole based bent-core liquid crystals. Liquid Crystals, 2015, 42, 1754-1764.	0.9	21
129	Polymer Solar Cells: Solubility Controls Fiber Network Formation. Journal of the American Chemical Society, 2015, 137, 11783-11794.	6.6	133
130	Subâ€10 nm Features Obtained from Directed Selfâ€Assembly of Semicrystalline Polycarbosilaneâ€Based Block Copolymer Thin Films. Advanced Materials, 2015, 27, 261-265.	11.1	63
131	Probing polymer crystallization at processing-relevant cooling rates with synchrotron radiation. AIP Conference Proceedings, 2015, , .	0.3	Ο
132	Structure Development of Low-Density Polyethylenes During Film Blowing: A Real-Time Wide-Angle X-ray Diffraction Study. Macromolecular Materials and Engineering, 2014, 299, 1494-1512.	1.7	32
133	A high pressure cell for supercritical CO2 on-line chemical reactions studied with x-ray techniques. Review of Scientific Instruments, 2014, 85, 093905.	0.6	17
134	Effect of the <i>Ortho</i> Alkylation of Perylene Bisimides on the Alignment and Selfâ€Assembly Properties. ChemistryOpen, 2014, 3, 138-141.	0.9	13
135	Synchrotron based in situ characterization during atomic layer deposition. , 2014, , .		0
136	Influence of metal–support interaction on the surface structure of gold nanoclusters deposited on native SiOx/Si substrates. Physical Chemistry Chemical Physics, 2014, 16, 6649.	1.3	25
137	Kinetics of Cross-Nucleation in Isotactic Poly(1-butene). Macromolecules, 2014, 47, 870-873.	2.2	47
138	Evidence of Cybotactic Order in the Nematic Phase of a Main-Chain Liquid Crystal Polymer with Bent-Core Repeat Unit. ACS Macro Letters, 2014, 3, 91-95.	2.3	29
139	Self-nucleation of isotactic poly(1-butene) in the trigonal modification. Polymer, 2014, 55, 137-142.	1.8	78
140	Morphology and local organization of water-containing (1R,2S)-dodecyl(2-hydroxy-1-methyl-2-phenylethyl)dimethylammonium bromide reverse micelles dispersed in toluene. Journal of Chemical Physics, 2014, 141, 084904.	1.2	2
141	Dynamic Behavior of Supramolecular Comb Polymers Consisting of Poly(2â€Vinyl Pyridine) and Palladiumâ€Pincer Surfactants in the Solid State. Chemistry - A European Journal, 2014, 20, 6951-6959.	1.7	4
142	Additive-assisted supramolecular manipulation of polymer:fullerene blend phase morphologies and its influence on photophysical processes. Materials Horizons, 2014, 1, 270-279.	6.4	58
143	X-ray irradiation induced reduction and nanoclustering of lead in borosilicate glass. CrystEngComm, 2014, 16, 9331-9339.	1.3	23
144	Hierarchical Structures of Polystyrene-block-poly(2-vinylpyridine)/Palladium–Pincer Surfactants: Effect of Weak Surfactant–Polymer Interactions on the Morphological Behavior. Macromolecules, 2014, 47, 5774-5783.	2.2	13

#	Article	IF	CITATIONS
145	Form l′ crystal formation in random butene-1/propylene copolymers as revealed by real-time X-ray scattering using synchrotron radiation and fast scanning chip calorimetry. European Polymer Journal, 2014, 60, 22-32.	2.6	46
146	Flow induced crystallization in isotactic polypropylene during and after flow. Polymer, 2014, 55, 6140-6151.	1.8	45
147	Formation and Growth of Pd Nanoparticles Inside a Highly Cross-Linked Polystyrene Support: Role of the Reducing Agent. Journal of Physical Chemistry C, 2014, 118, 8406-8415.	1.5	37
148	Kinetics of the Polymorphic Transition in Isotactic Poly(1-butene) under Uniaxial Extension. New Insights From Designed Mechanical histories Macromolecules, 2014, 47, 3033-3040.	2.2	69
149	Unusual crystallization behavior of isotactic polypropylene andÂpropene/1-alkene copolymers at large undercoolings. Polymer, 2014, 55, 3234-3241.	1.8	23
150	Patterned Silver Nanoparticles embedded in a Nanoporous Smectic Liquid Crystalline Polymer Network. Journal of the American Chemical Society, 2013, 135, 10922-10925.	6.6	38
151	On cross- and self-nucleation in seeded crystallization of isotactic poly(1-butene). Polymer, 2013, 54, 4637-4644.	1.8	59
152	Small-Angle X-Ray Scattering for the Study of Nanostructures and Nanostructured Materials. , 2013, , 175-228.		2
153	Microstructure, state of water and proton conductivity of sulfonated poly(ether ether ketone). Solid State Ionics, 2013, 252, 62-67.	1.3	13
154	Microfocus wide-angle X-ray scattering of polymers crystallized in a fast scanning chip calorimeter. Thermochimica Acta, 2013, 563, 33-37.	1.2	75
155	Crystallization-Driven Enhancement in Photovoltaic Performance through Block Copolymer Incorporation into P3HT:PCBM Blends. Macromolecules, 2013, 46, 3015-3024.	2.2	38
156	Dynamics of Magnetic Alignment in Rod–Coil Block Copolymers. Macromolecules, 2013, 46, 4462-4471.	2.2	34
157	Influence of Solid-State Microstructure on the Electronic Performance of 5,11-Bis(triethylsilylethynyl) Anthradithiophene. Chemistry of Materials, 2013, 25, 1823-1828.	3.2	21
158	A Critical Revision of the Nanoâ€Morphology of Proton Conducting Ionomers and Polyelectrolytes for Fuel Cell Applications. Advanced Functional Materials, 2013, 23, 5390-5397.	7.8	273
159	Short-Term Flow Induced Crystallization in Isotactic Polypropylene: How Short Is Short?. Macromolecules, 2013, 46, 9249-9258.	2.2	64
160	Side Chains Control Dynamics and Self-Sorting in Fluorescent Organic Nanoparticles. ACS Nano, 2013, 7, 408-416.	7.3	58
161	Polymer crystallization studies under processing-relevant conditions at the SAXS/WAXS DUBBLE beamline at the ESRF. Journal of Applied Crystallography, 2013, 46, 1681-1689.	1.9	111
162	Shearâ€Induced Orientation of Gyroid PSâ€ <i>b</i> â€P4VP(PDP) Supramolecules. Macromolecular Rapid Communications, 2013, 34, 1208-1212.	2.0	10

#	Article	IF	CITATIONS
163	Crystallization of a Polyamide 6/Montmorillonite Nanocomposite at Rapid Cooling. Macromolecular Materials and Engineering, 2013, 298, 938-943.	1.7	26
164	Double Gyroid Network Morphology in Supramolecular Diblock Copolymer Complexes. Macromolecules, 2012, 45, 3503-3512.	2.2	47
165	Increase in short-chain ceramides correlates with an altered lipid organization and decreased barrier function in atopic eczema patients. Journal of Lipid Research, 2012, 53, 2755-2766.	2.0	349
166	The influence of charge ratio on transient networks of polyelectrolyte complex micelles. Soft Matter, 2012, 8, 104-117.	1.2	34
167	Sedimentation and depletion attraction directing glass and liquid crystal formation in aqueous platelet/sphere mixtures. Soft Matter, 2012, 8, 191-197.	1.2	26
168	Nanostructure Development in Alkoxide-Carboxylate-Derived Precursor Films of Barium Titanate. Journal of Physical Chemistry C, 2012, 116, 425-434.	1.5	10
169	Structure of singly terminated polar DyScO <mml:math xmlns:mml="http://www.w3.org/1998/Math/MathML" display="inline"&gt;<mml:msub><mml:mrow /&gt;<mml:mn>3</mml:mn></mml:mrow </mml:msub>(110) surfaces. Physical Review B, 2012, 85, .</mml:math 	1.1	17
170	Mesophase-Mediated Crystallization of Poly(butylene-2,6-naphthalate): An Example of Ostwald's Rule of Stages. ACS Macro Letters, 2012, 1, 1051-1055.	2.3	47
171	Exploring the Origin of Crystalline Lamella Twist in Semi-Rigid Chain Polymers: the Model of Keith and Padden revisited. Macromolecules, 2012, 45, 7454-7460.	2.2	69
172	Block Copolymer as a Nanostructuring Agent for Highâ€Efficiency and Annealingâ€Free Bulk Heterojunction Organic Solar Cells. Advanced Materials, 2012, 24, 2196-2201.	11.1	71
173	Effect of reduction in liquid phase on the properties and the catalytic activity of Pd/Al2O3 catalysts. Journal of Catalysis, 2012, 287, 44-54.	3.1	62
174	Structural Characterization of Surfactant-Coated Bimetallic Cobalt/Nickel Nanoclusters by XPS, EXAFS, WAXS, and SAXS. Journal of Physical Chemistry C, 2011, 115, 6360-6366.	1.5	39
175	Aggregation of Ureido-Pyrimidinone Supramolecular Thermoplastic Elastomers into Nanofibers: A Kinetic Analysis. Macromolecules, 2011, 44, 6776-6784.	2.2	163
176	Increased Order–Disorder Transition Temperature for a Rod–Coil Block Copolymer in the Presence of a Magnetic Field. Macromolecules, 2011, 44, 7503-7507.	2.2	17
177	Attractive glass formation in aqueous mixtures of colloidal gibbsite platelets and silica spheres. Soft Matter, 2011, 7, 2832.	1.2	20
178	Lamellar Lipid Organization and Ceramide Composition in the Stratum Corneum of Patients with Atopic Eczema. Journal of Investigative Dermatology, 2011, 131, 2136-2138.	0.3	96
179	Nanoscale Structure Evolution in Alkoxide–Carboxylate Sol–Gel Precursor Solutions of Barium Titanate. Journal of Physical Chemistry C, 2011, 115, 20449-20459.	1.5	16
180	Effect of cooling rate on the crystal/mesophase polymorphism of polyamide 6. Colloid and Polymer Science, 2011, 289, 1073-1079.	1.0	83

#	Article	IF	CITATIONS
181	In situ X-ray analysis of mesophase formation in random copolymers of propylene and 1-butene. Polymer Bulletin, 2011, 67, 497-510.	1.7	24
182	Exploring the structure of inter-platelet galleries in organically modified montmorillonite using the small-angle X-ray scattering interface distribution function approach. Journal of Applied Crystallography, 2011, 44, 805-811.	1.9	3
183	On the origin of the "coreâ€free―morphology in microinjectionâ€molded HDPE. Journal of Polymer Science, Part B: Polymer Physics, 2011, 49, 1470-1478.	2.4	39
184	Controlled Supramolecular Oligomerization of <i>C<sub>3</sub></i> â€Symmetrical Molecules in Water: The Impact of Hydrophobic Shielding. Chemistry - A European Journal, 2011, 17, 5193-5203.	1.7	51
185	The effect of n-, s- and t-butanol on the micellization and gelation of Pluronic P123 in aqueous solution. Journal of Colloid and Interface Science, 2011, 353, 482-489.	5.0	9
186	Combined time-resolved SAXS and X-ray Spectroscopy methods. Journal of Physics: Conference Series, 2010, 247, 012047.	0.3	6
187	Influence of shear in the crystallization of polyethylene in the presence of SWCNTs. Carbon, 2010, 48, 4116-4128.	5.4	35
188	Investigation of the Micellization in Thin Films Using Resonant Soft X-Ray Scattering. IOP Conference Series: Materials Science and Engineering, 2010, 14, 012017.	0.3	3
189	Controlling the growth and shape of chiral supramolecular polymers in water. Proceedings of the National Academy of Sciences of the United States of America, 2010, 107, 17888-17893.	3.3	194
190	Following the Synthesis of Metal Nanoparticles within pH-Responsive Microgel Particles by SAXS. Macromolecules, 2010, 43, 9828-9836.	2.2	22
191	A Study on the Chainâ^'Particle Interaction and Aspect Ratio of Nanoparticles on Structure Development of a Linear Polymer. Macromolecules, 2010, 43, 6749-6759.	2.2	57
192	Real-Time WAXD Detection of Mesophase Development during Quenching of Propene/Ethylene Copolymers. Macromolecules, 2010, 43, 10208-10212.	2.2	73
193	Diffuse scattering in random-stacking hexagonal close-packed crystals of colloidal hard spheres. Phase Transitions, 2010, 83, 107-114.	0.6	19
194	Combined small-angle x-ray scattering/extended x-ray absorption fine structure study of coated Co nanoclusters in bis(2-ethylhexyl)sulfosuccinate. Journal of Applied Physics, 2009, 105, 114308.	1.1	8
195	Influence of Nanoparticles on the Rheological Behaviour and Initial Stages of Crystal Growth in Linear Polyethylene. Macromolecular Chemistry and Physics, 2009, 210, 2174-2187.	1.1	18
196	Micellization of Miktoarm Star S <sub><i>n</i></sub> I <sub><i>n</i></sub> Copolymers in Block Copolymer/Homopolymer Blends. Macromolecules, 2009, 42, 5285-5295.	2.2	13
197	Molecular Organization of Cylindrical Sexithiophene Aggregates Measured by X-ray Scattering and Magnetic Alignment. Langmuir, 2009, 25, 1272-1276.	1.6	13
198	Triblock Protein Copolymers Forming Supramolecular Nanotapes and pH-Responsive Gels. Macromolecules, 2009, 42, 1002-1009.	2.2	59

#	Article	IF	CITATIONS
199	Protein stability modulated by a conformational effector: effects of trifluoroethanol on bovine serum albumin. Physical Chemistry Chemical Physics, 2009, 11, 4007.	1.3	46
200	Segmental Orientation in Well-Defined Thermoplastic Elastomers Containing Supramolecular Fillers. Macromolecules, 2009, 42, 524-530.	2.2	34
201	Poly(p-phenylene sulfone)s with high ion exchange capacity: ionomers with unique microstructural and transport features. Physical Chemistry Chemical Physics, 2009, 11, 3305.	1.3	110
202	The incorporation of rigid diol monomers into poly(butylene terephthalate) via solidâ€state copolymerization and melt copolymerization. Journal of Polymer Science Part A, 2008, 46, 1203-1217.	2.5	19
203	Disk micelles from amphiphilic Janus gold nanoparticles. Chemical Communications, 2008, , 697-699.	2.2	42
204	Thermoreversible DMDBS Phase Separation in iPP: The Effects of Flow on the Morphology. Macromolecules, 2008, 41, 5350-5355.	2.2	45
205	Synthesis, Structure, and Properties of Ionic Thermoplastic Elastomers Based on Maleated Ethylene/Propylene Copolymers. Macromolecules, 2008, 41, 5493-5501.	2.2	37
206	Structural Characterization of Frozen <i>n</i> -Heptane Solutions of Metal-Containing Reverse Micelles. Langmuir, 2007, 23, 11482-11487.	1.6	18
207	Small-angle energy-dispersive X-ray scattering using a laboratory-based diffractometer with a conventional source. Journal of Applied Crystallography, 2007, 40, 218-231.	1.9	4
208	Large size fibrillar bundles of the Alzheimer amyloid β-protein. European Biophysics Journal, 2007, 36, 701-709.	1.2	13
209	Sulphonated poly(ether ether ketone) membranes for fuel cell application: Thermal and structural characterisation. Journal of Power Sources, 2006, 163, 18-26.	4.0	122
210	Structural and electrochemical investigation on re-cast Nafion membranes for polymer electrolyte fuel cells (PEFCs) application. Journal of Membrane Science, 2006, 278, 105-113.	4.1	59
211	Energy-dispersive small-angle x-ray scattering for investigating polymer morphology: Static and time-resolved experiments. Applied Physics Letters, 2004, 85, 4798-4800.	1.5	3